Is Handheld Optical Coherence Tomography Reliable in Infants and Young Children With and Without Nystagmus?

Helena Lee, Frank Proudlock, and Irene Gottlob

Ophthalmology Group, University of Leicester, Robert Kilpatrick Clinical Sciences Building, Leicester Royal Infirmary, Leicester, United Kingdom

Correspondence: Irene Gottlob, Ophthalmology Group, University of Leicester, Robert Kilpatrick Clinical Sciences Building, PO Box 65, Leicester Royal Infirmary, Leicester LE2 7LX, UK; ig15@leicester.ac.uk.

HL and FP are joint first authors.

Submitted: September 9, 2013
Accepted: November 2, 2013

Citation: Lee H, Proudlock F, Gottlob I. Is handheld optical coherence tomography reliable in infants and young children with and without nystagmus? *Invest Ophthalmol Vis Sci*. 2013;54:8152–8159. DOI:10.1167/iovs.13-13230

Purpose. To evaluate the reliability of the spectral domain handheld OCT (HH-OCT) in assessing foveal morphology in children with and without nystagmus.

Methods. Forty-nine subjects with nystagmus (mean age 43.83 months; range, 1–82 months) and 48 controls (mean age 43.02 months; range, 0 to 83 months) were recruited and scanned using HH-OCT. A minimum of two separate volumetric scans on the same examination day of the fovea were obtained. The images were imported into ImageJ software where manual retinal layer segmentation of the central foveal B-scan was performed. Agreement between scans was assessed by determining the intraclass correlation coefficients (ICC) and Bland-Altman plots.

Results. Both the nystagmus and control groups showed an excellent degree of reproducibility between two examinations with ICCs greater than 0.96 for central macular thickness (CMT) and greater than 0.8 for the outer nuclear layer and outer segment of the photoreceptors. The nerve fiber layer, ganglion cell layer, outer plexiform layer, inner segment of the photoreceptors, and retinal pigment epithelium were less reliable with ICCs of less than 0.7. There was no difference in the reliability of scans obtained in children with nystagmus as compared with controls and both groups had good intereye agreement with ICCs greater than 0.94 for CMT.

Conclusions. We have shown for the first time that the HH-OCT provides reliable measurements in children with and without nystagmus. This is important, as the HH-OCT will have a greater diagnostic and prognostic role in young children with nystagmus and other eye diseases in the future.

Keywords: optical coherence tomography, congenital nystagmus, children, fovea, reliability

Although optical coherence tomography (OCT) has revolutionized diagnosis and treatment in many retinal diseases in adults and older children, infants and children too small to cooperate have been deprived clinically from OCT. A handheld spectral domain OCT (HH-OCT), which has been optimized for use in infants and young children, has demonstrated its clinical utility in identifying retinal morphology in infants with retinopathy of prematurity (ROP), maculopathy, retinal dystrophy, posttraumatic choroidal neovascularization, and Leber's congenital amaurosis.[1–8] We have recently shown that the HH-OCT is reliable for diagnosing the etiology of nystagmus.[9]

In older patients with nystagmus, it has been shown that OCT produces reliable retinal measurements and can differentiate albinism, changes in PAX6 mutation, and achromatopsia from idiopathic nystagmus by identifying typical or atypical foveal hypoplasia.[10–12] It also has been shown that the length of the photoreceptor outer segment is a strong predictor of visual acuity in patients with albinism.[11] It has been reported that the images obtained using HH-OCT contain movement artifacts caused by the examiner and/or the child.[8] Also, it is unclear if reliable measurements of the retinal layers can be obtained using the HH-OCT in infants and young children with and without nystagmus. In this study, we evaluated the reliability of the HH-OCT in assessing foveal morphology in healthy children and children with nystagmus, likely to be one of the most difficult pathologies to image, aged between birth and 6 years.

Patients and Methods

The cohort for this study included 49 children with nystagmus (mean age 43.83 months; SD 24.1 months; range, 1–82 months) and 48 control participants (mean age 43.02 months; SD 24.7 months; range, 0–83 months) in which a minimum of two separate successful OCT scans on at least one eye were obtained on the same day. The demographic data and diagnostic breakdown are summarized in Table 1.

Spectral domain HH-OCT (Bioptigen Envisu system; Bioptigen, Durham, NC) was used to obtain a minimum of two separate volumetric scans (consisting of 100 B scans and 500 A scans per B scan) on the same examination day of the foveal region. The acquisition speed for each B scan was 5.8 ms with an overall scan time of 2.9 seconds and a digital resolution of 2.4 μm per pixel. This ensured that any motion artifact caused by nystagmus was minimal. All children were scanned in the outpatient clinic setting without sedation. A total of 166 scans in the nystagmus participants and 164 scans in the healthy controls were obtained. Repeat scans were obtained in at least one eye in all nystagmus subjects ($n = 49$) and all healthy controls ($n = 48$). Acquisition of an OCT scan was considered

Table 1. Summary of Demographic Data and Diagnostic Category of Participants

Category	Age Range, mo	Mean Age, mo (SD)	Sex, *n*		Eye Analyzed, *n*	
			Male	Female	Right	Left
Control, $n = 48$	0–83	43.83 (24.69)	25	23	33	15
Albinism, $n = 27$	1–82	41.81 (22.93)	17	10	20	7
IIN, $n = 11$	7–81	43.82 (28.06)	10	1	6	5
Achromatopsia, $n = 4$	2–70	27.25 (30.02)	2	2	1	3
Patients with PAX6 mutations, $n = 3$	48–76	59.67 (14.57)	2	1	2	1
Retinal dystrophy, $n = 3$	45–77	57.67 (17.01)	2	1	3	—
Latent nystagmus, $n = 1$	—	36	1	—	1	—

Dashes indicate nonapplicable or none. IIN, idiopathic infantile nystagmus; *n*, sample size.

successful if the B scan containing the foveal center was captured together with a minimum of five uninterrupted B scans (i.e., without refixations or blinks on either side of the central foveal B scan). The retinal vasculature and optic nerve head were used to determine if refixations had taken place during the scan.

The acquired images were exported from the Bioptigen OCT software and imported into ImageJ software (available in the public domain at http://rsbweb.nih.gov/ij/; National Institutes of Health, Bethesda, MD) where retinal layer segmentation was performed by manually identifying each layer at the fovea (Fig. 1). The fovea was identified by visual inspection of the B-scan images for the presence of a foveal depression, thinning of the inner retinal layers, doming of the outer nuclear layer, and lengthening of the photoreceptor outer segments, as described by Mohammad et al.[11] Measurements of each retinal layer were performed only if the borders between each adjacent retinal layer were visible. In cases in

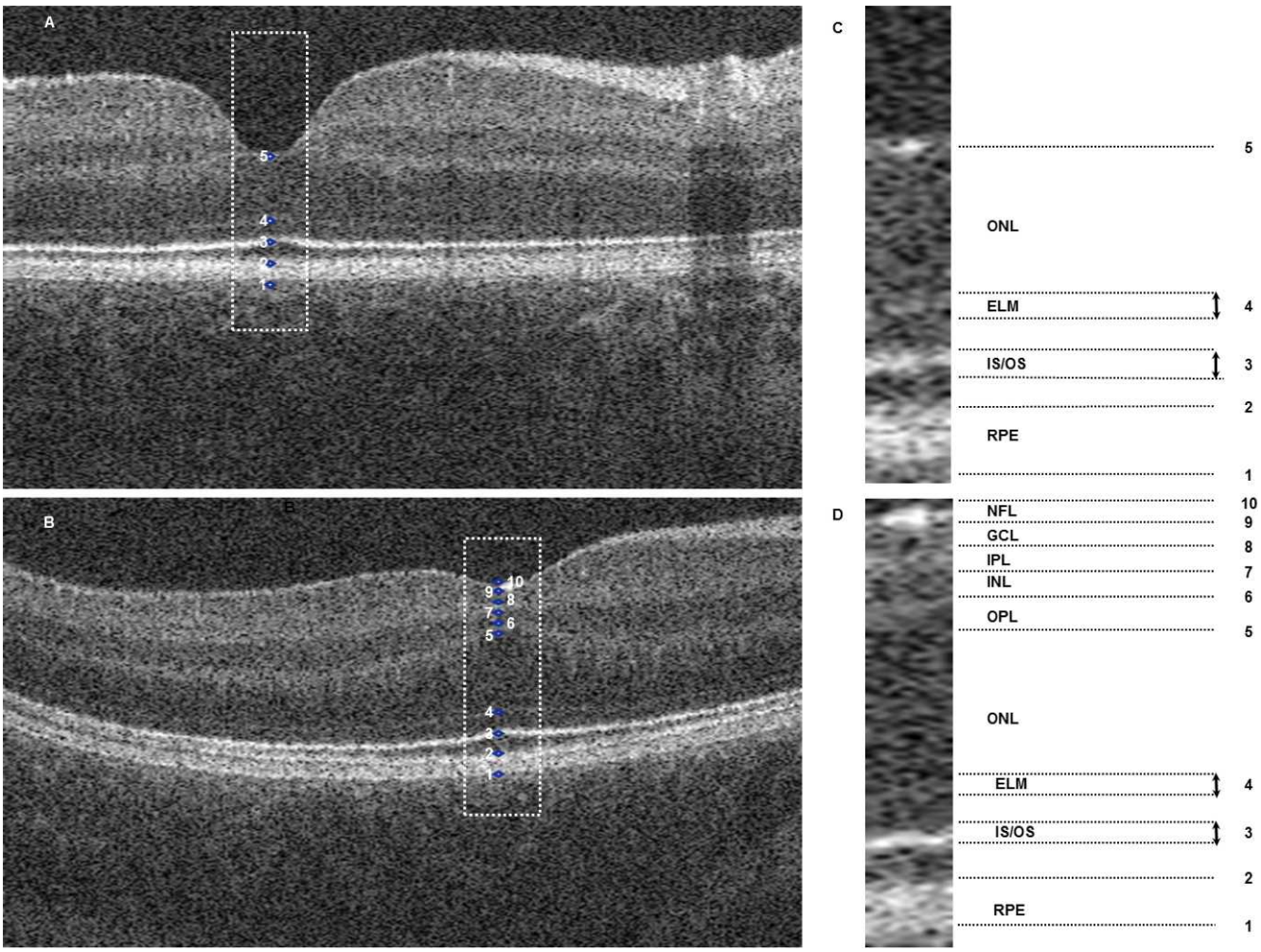

Figure 1. Optical coherence tomograms of one control subject (**A**) and one nystagmus subject (**B**). Segmentation of the foveal B scans was performed using ImageJ software, which identified 10 points (**C**, **D**). These points represented the following: 1 to 2 = RPE; 2 to 3 = OS; 3 = IS/OS junction; 3 to 4 = IS; 4 ELM; 4 to 5 = ONL; 5 to 6 = OPL; 6 to 7 = INL; 7 to 8 = IPL; 8 to 9 = GCL; 9 to 10 = NFL.

Investigative Ophthalmology & Visual Science

Investigative Ophthalmology & Visual Science

TABLE 2. Reproducibility of First to Second Scan Measurements of Each Outer Retinal Layer

	Control, $n = 48$ for ICC of Repeated Measures From 1 Eye; $n = 45$ for ICC of Intereye Comparison							Nystagmus, $n = 49$ for ICC of Repeated Measures From 1 Eye; $n = 47$ for ICC of Intereye Comparison						
	Clear		Not Clear		Not Visible		Not Present	Clear		Not Clear		Not Visible		Not Present
Retinal Layer	ICC, *n*	Intereye, *n*	ICC, *n*	Intereye, *n*	ICC, *n*	Intereye, *n*	ICC, *n*	Intereye, *n*	ICC, *n*	Intereye, *n*	ICC, *n*	Intereye, *n*	ICC, *n*	Intereye, *n*
CMT	0.960, 47	0.947, 44	1	1	0	0	0	0	0.966, 42	0.987, 40	0.982, 6	0.341, 7	1	0	0	0
ONL	0.887, 31	0.820, 19	0.928, 16	0.808, 24	1	1	0	1	0.932, 22	0.877, 12	0.858, 25	0.873, 32	2	3	0	0
IS	0.557, 33	0.517, 25	0.367, 12	0.704, 17	3	3	0	0	0.626, 20	0.583, 12	0.289, 18	0.699, 22	6	8	5	5
ONL and IS	0.931, 46	0.897, 44	2	1	0	0	0	0	0.931, 35	0.878, 29	0.633, 9	0.911, 13	2	2	3	3
OS	0.872, 38	0.695, 36	0.343, 8	0.426, 8	0	0	2	1	0.828, 33	0.742, 26	0.588, 9	0.816, 12	1	33	6	6
RPE	0.305, 39	0.501, 36	0.822, 9	0.7, 9	0	0	0	0	0.671, 36	0.624, 29	0.687, 13	0.560, 18	0	0	0	0
OS and RPE	0.870, 48	0.914, 45	0	0	0	0	0	0	0.933, 49	0.943, 47	0	0	0	0	0	0

The data from one eye of each subject was classified into one of four categories based on border clarity. If there was a difference in the classification of the first and second scan data sets from the same eye, then that eye was placed in the lower-quality category. The ICCs were calculated only where $n > 5$. The intereye correlation also is shown for each retinal layer for both groups. Clear = Borders of the retinal layer can be delineated accurately. Not Clear = Borders of the retinal layer are visible but indistinct making delineation inaccurate. Not Visible = Retinal layer is visible but the delineating borders are not visible. Not Present = Retinal layer is not present.

which the border between adjacent retinal layers was not clear a combined measurement of the affected layers was taken (see first section of Results).

We analyzed the reproducibility of retinal layer measurements between separate scans of each participant, the difference in reliability between scans obtained in children with nystagmus as compared with age-matched controls, and the intereye agreement on scans obtained from the same subject. Reproducibility between scans was assessed by determining the intraclass correlation coefficient (ICC) and by Bland-Altman assessment. For the test–retest analysis, if repeat scans were present for both eyes, only a single eye (the right eye) was analyzed. If two repeated scans were available for only one eye, this eye was chosen. A summary of the total number of right and left eyes analyzed is provided in Table 1. If more than two scans were obtained, the two highest-quality scans were selected for analysis, with the highest-quality scan analyzed first so that any bias due to quality of the scan is shown by the test–retest analysis. We determined the quality of each scan based on the clarity of the borders of each retinal layer (Tables 2, 3). A paired-samples *t*-test was conducted to determine the effects of age on the reliability of the retinal measurements.

All analyses were considered significant at a type 1 probability value of P less than 0.05. Statistical analysis was performed with SPSS software version 16.0 (SPSS, Inc., Chicago, IL).

The study adhered to the tenets of the Declaration of Helsinki and was approved by the local ethics committee. Informed consent was obtained from all parents/guardians of patients and control subjects participating in this study.

RESULTS

Segmentation Difficulties

There were several borders between retinal layers that were not easy to identify in a subset of participants. These were as follows:

- The external limiting membrane (ELM), that is, the border between the outer nuclear layer (ONL) and inner segment of the photoreceptors (IS), was difficult to identify clearly in 15 (31.2%) of 48 analyzed eyes in control participants. In 24 (49%) of 49 analyzed eyes in participants with nystagmus, the ELM was difficult to identify in the foveal area (Table 2; Figs. 2C, 2D). Five of the 49 participants with nystagmus were achromats in whom the IS was disrupted by a hyporeflective zone and therefore could not be analyzed. The ELM appeared more difficult to identify in the younger participants in both groups. The mean age at which the ELM was clearly identified was 53.25 months and 45.61 months in the nystagmus and control groups, respectively. In comparison with this, the mean age of the participants in whom the ELM was not visible was 23.17 months and 18.67 months in the nystagmus and control groups, respectively. However, the effect of age was not significant in either the control participants ($P = 0.596$) or the nystagmus participants ($P = 0.093$).
- The border between the outer segment of the photoreceptors (OS) and the retinal pigment epithelium (RPE), although present on all scans, was often indistinct, preventing accurate demarcation (for example see magnified region of Fig. 2H). Consequently, it was difficult to identify the border in 9 (18.8%) of 48 analyzed eyes in control participants and in 13 (26.5%) of 49 analyzed eyes in participants with nystagmus

Table 3. Reproducibility of First to Second Scan Measurements of Each Inner Retinal Layer

	Nystagmus, $n = 49$ for ICC of Repeated Measures From 1 Eye; $n = 47$ for ICC of Intereye Comparison							
	Clear		Not Clear		Not Visible		Not Present	
Retinal Layer	ICC, *n*	Intereye, *n*	ICC, *n*	Intereye, *n*	ICC, *n*	Intereye, *n*	ICC, *n*	Intereye, *n*
NFL	0.481, 24	0.721, 20	2	0.369, 5	1	1	22	21
GCL	0.623, 14	0.750, 9	−0.313, 12	0.581, 14	2	3	21	21
IPL	0.741, 16	0.781, 10	0.425, 13	0.218, 15	4	6	16	16
GCL and IPL	0.870, 24	0.819, 19	4	0.833, 6	3	4	18	18
INL	0.778, 23	0.760, 18	0.602, 5	0.684, 6	5	7	16	16
OPL	0.401, 21	0.536, 13	0.845, 7	0.597, 10	5	8	16	16

The data from one eye of each subject was classified into one of four categories based on border clarity. If there was a difference in the classification of the first and second scan data sets from the same eye, then that eye was placed in the lower-quality category. The ICCs were calculated only where $n > 5$. The intereye correlation is also shown for each retinal layer for both groups. Clear = Borders of the retinal layer can be delineated accurately. Not Clear = Borders of the retinal layer are visible but indistinct making delineation inaccurate. Not Visible = Retinal layer is visible but the delineating borders are not visible. Not Present = Retinal layer is not present.

(Table 3). The mean age at which this border was clearly identified was 44.75 months and 49.26 months in the nystagmus and control groups, respectively. In comparison, the mean age of the participants in whom this border was not clear was 38.23 months and 20.33 months in the nystagmus and control groups, respectively. This border was significantly more difficult to delineate in the younger participants of the control group ($P = 0.029$). The effect of age did not reach significance in the nystagmus group ($P = 0.097$).

- In the case of foveal hypoplasia, in the nystagmus group, the border between the ganglion cell layer (GCL) and inner plexiform layer (IPL) could be difficult to identify. The border was not clearly visible in 14 (50%) of the 28 participants with foveal hypoplasia in whom these layers were present (Table 3; Figs. 2C, 2G). There was no significant age difference between any of the segmentation categories of this group ($P = 0.574$). This border could be visualized clearly in 43.2% and 50% of the albinism and PAX6 participants, respectively. This was most difficult to identify in achromatopsia, with the border being clearly identified in only 25% of the achromatopsia participants.

We have provided measurements of the combined layers, IS-ONL, OS-RPE, and GCL-IPL, in Tables 2 and 3 in order to take the difficulties with accurate segmentation of these borders into account.

Reproducibility of Retinal Measurements Between Scans

Both the nystagmus and control groups demonstrated excellent reproducibility between two examinations for central macular thickness (CMT) with ICCs greater than 0.96.

In general, measurement of the outer retinal layers showed a good degree of reproducibility with ICCs of between 0.8 and 0.95 for the ONL, OS, combined ONL-IS, and combined OS-RPE measurements in both the nystagmus and control groups. The test–retest reliability of the IS and RPE measurements were not as consistent, with ICCs of 0.626 and 0.671, respectively, in the nystagmus group. The ICCs were 0.557 and 0.305, respectively, in the control group.

For the inner retinal layers that were present in the fovea in patients with foveal hypoplasia in the nystagmus group, there was a good degree of reproducibility for the IPL, INL, and combined GCL- IPL measurements with ICCs of 0.741, 0.778, and 0.870, respectively. The test–retest reliability of the other inner retinal layers, the nerve fiber layer (NFL), GCL, and outer plexiform layer (OPL), was not as consistent with ICCs of 0.481, 0.623, and 0.401, respectively. The ICCs were comparable between both groups, showing that there is no difference in the reliability of scans obtained in children with nystagmus as compared with age-matched healthy controls (Tables 2, 3).

Intereye Comparison of Nystagmus and Control Subjects

Scans of both eyes were compared in 47 of the nystagmus subjects and 45 of the control subjects. Both the nystagmus and control groups showed a good degree of intereye agreement with ICCs greater than 0.94 for CMT (Tables 2, 3; Fig. 1C).

Bland-Altman Assessment

A Bland-Altman assessment for agreement was used to compare the two separate measurements (Table 4). With the exception of the CMT and combined OS-RPE measurements in the control group and the INL, OPL, and combined OS-RPE measurements in the nystagmus group, bias was not significantly different from zero in both groups for all retinal layer measurements.

There was a significant positive bias in the CMT and combined OS-RPE measurements in the control group with a biases of 0.291 ($P = 0.044$) and 0.484 ($P < 0.0001$), respectively, indicating a trend toward larger-thickness measurements for these layers with better-quality scans. There was also a significant positive bias in the OS and combined OS-RPE measurement in the nystagmus group with a bias of 0.402 ($P = 0.008$) and 0.647 ($P < 0.0001$), respectively, indicating a trend toward a larger-thickness measurement for this layer with higher-quality scans.

There was a significant negative bias in the measurements if the INL and OPL in the nystagmus group, with biases of –0.615 ($P < 0.000$) and –0.609 ($P = 0.001$), respectively, indicating a trend toward smaller-thickness measurements for these layers with higher-quality scans.

The 95% limits of agreement that were established ranged from a minimum interval of –1.0 to 2.8 for the OS, a maximum interval of –3.2 to 3.4 for the ONL in the control group, a minimum interval of –1.7 to 2.2 for the RPE, and a maximum interval of –6.7 to 5.4 for the combined ONL and IS measurement in the nystagmus group. The limits of agreement were narrower in the control as compared with the patient

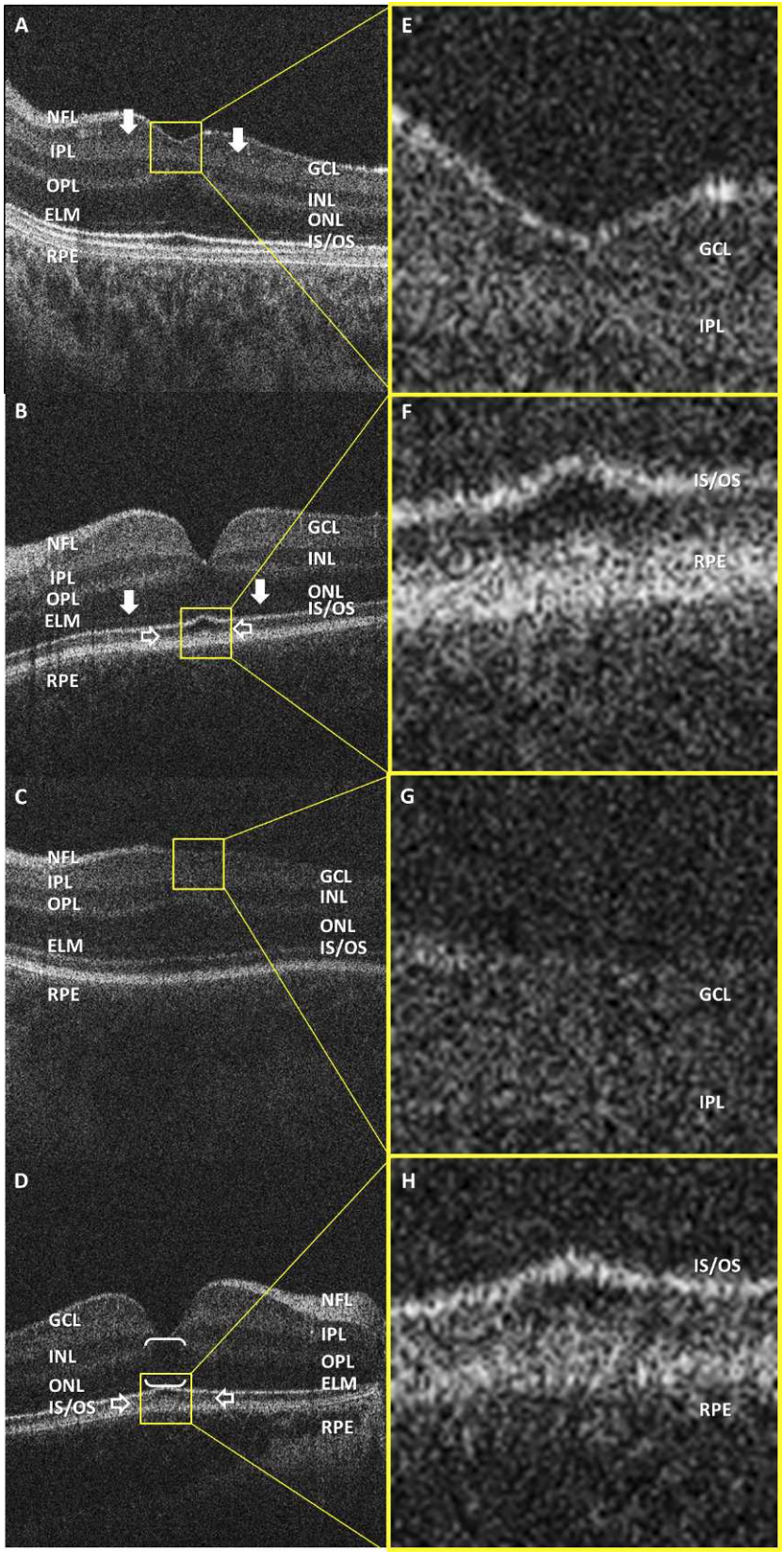

Figure 2. Optical coherence tomograms of 2 nystagmus subjects (**A**, **C**) and 2 control subjects (**B**, **D**). Examples of the difficulties encountered in the segmentation of the retinal layers are shown. The border between the GCL and IPL (indicated by the *arrows* in [**A**]) is often difficult to identify. If the border between these layers could not be delineated, then a combined measurement was taken from the GCL and IPL. A magnified section of the GCL and IPL in (**B**, **D**), which is indicated by the *yellow box*, is shown in (**A**, **C**).The ELM (indicated by the *arrows* in [**B**]) is often difficult to delineate (**D**). If the ELM could not be identified, then a combined measurement was taken from the ONL and IS. The upper border of the RPE

Investigative Ophthalmology & Visual Science

(indicated by the *open arrows* in [**B**, **D**]) can be nondistinct (**D**). If this occurred, then a combined measurement was taken from the OS and RPE. A magnified section of the border between the OS and RPE, as indicated by the *yellow box* in (**B**) and (**D**) is shown in (**F**) and (**H**), respectively.

group. The limits of agreement between patients and controls are of similar ranges and small enough for clinical tests.

Discussion

We have demonstrated for the first time that the HH-OCT produces reliable assessments of foveal morphology in young children with and without nystagmus. The ICCs for CMT were excellent, with an ICC of 0.966 in the nystagmus group and 0.960 in the control group. These are only marginally lower than those obtained in adult patients with nystagmus (0.97) and adult controls (0.98).[12] This should be expected, as the inner limiting membrane (ILM) and Bruch's membrane exhibit the strongest signals on OCT. The ICCs for ONL and OS also were high, with ICCs greater than 0.8 in the nystagmus and in the control group, respectively. Reliable quantification of the OS is important clinically, as this can potentially be used as an objective predictor of visual acuity.[11] Bland-Altman plots showed good agreement for both groups for intraretinal thickness measurements and the 95% limits of agreement were comparable with those reported in adults with and without nystagmus.[12]

We have also identified which retinal layers may be less reliable when quantified. This includes the GCL and OPL layers in the nystagmus group and the IS and RPE layers in both the nystagmus and control groups. The GCL and OPL layers have very similar reflectance profiles, making their borders more difficult to delineate accurately. This leads to a poor signal-to-noise ratio when image quality is not be of sufficient standard to allow accurate quantification of these layers.

Comparing the consistency of measurements based on whether the borders between individual layers are clear or not clear did improve the ICCs for the IS from 0.289 to 0.626 in the nystagmus group and from 0.367 to 0.557 in the control group. However the ICCs did not reach the same level of reliability as the other retinal layers, such as ONL. Also, comparing the consistency of measurements based on border clarity did not improve the ICCs for the OPL in the nystagmus group and the RPE in both the nystagmus and control groups. As these layers are much thinner than the other layers of the fovea, their measurements are likely to be more sensitive to errors, such as measurement error and quantization effects. The ICCs obtained in this study were higher, with the thicker retinal layers making this a plausible explanation.

One other explanation that would need to be considered is that in infants and young children the retinal layers are developing. Histological studies of the simian[13–15] and human[16,17] retina have demonstrated that macular development is a sophisticated process that involves the outward displacement of the inner retinal layers (GCL, INL, and IPL) and inward migration of the cone photoreceptors into the fovea. This process is thought not to be complete until between 11 months of age and 5 years.[16–19] Over time, the cone photoreceptors become taller, narrower, and more tightly packed as the fovea matures. It has been reported that the space between the ELM (which represents the ellipsoid of the inner segment of the photoreceptors[20]) and the RPE measures only 14 μm at the fovea at birth.[17] At 13 months of age, the length of the foveal IS/OS is 36 μm.[17] By 13 years of age, the photoreceptors have reached adult values, with the foveal IS measuring between 168 μm and 189 μm and the OS measuring between 139 μm and 155 μm long.[17]

It is possible that in the immature retina, structures such as the ELM may not be visible on OCT until they have matured sufficiently. We observed a tendency toward more difficulties with segmentation of the ELM and the junction between the OS and RPE in the younger participants of both groups. This did not reach statistical significance for the ELM in both groups and for the junction between the OS and RPE in the nystagmus group. The effect of age did reach significance, however, for

Table 4. Summary of Bland-Altman Plot for Measurements of Each Retinal Layer

Control, $n = 48$				Nystagmus, $n = 49$			
Retinal Layer	**Mean, μm (SD)**	**95% Limits of Agreement**	**Bias (*P* Value)**	**Retinal Layer**	**Mean, μm (SD)**	**95% Limits of Agreement**	**Bias (*P* Value)**
CMT $n = 48$	192.100 (24.957)	−3.8 to 2.3	0.291 (0.044)*	CMT $n = 48$	240.908 (61.075)	−7.5 to 4.1	−0.066 (0.656)
NFL $n = 1$	—	—	—	NFL $n = 26$	9.479 (3.962)	−4.9 to 0.2	0.058 (0.777)
GCL $n = 1$	—	—	—	GCL $n = 26$	25.864 (8.288)	−4.3 to 6.4	0.092 (0.653)
IPL $n = 4$	—	—	—	IPL $n = 29$	30.552 (9.455)	−4.6 to 4.2	0.139 (0.472)
GCL and IPL $n = 1$	—	—	—	GCL and IPL $n = 28$	53.959 (20.355)	−6.4 to 4.4	0.290 (0.134)
INL $n = 4$	—	—	—	INL $n = 28$	53.959 (20.355)	−6.2 to 4.4	−0.615 (0.000)*
OPL $n = 4$	—	—	—	OPL $n = 28$	18.893 (8.069)	−5.3 to 1.4	−0.609 (0.001)*
ONL $n = 47$	96.049 (18.004)	−3.2 to 3.4	0.139 (0.350)	ONL $n = 47$	90.332 (22.557)	−5.2 to 3.8	0.080 (0.592)
IS $n = 45$	29.340 (5.234)	−3.5 to 0.8	−0.700 (0.648)	IS $n = 38$	26.871 (4.503)	−0.2 to 4.0	−0.830 (0.620)
ONL and IS $n = 45$	125.811 (20.261)	−3.9 to 2.6	0.196 (0.197)	ONL and IS $n = 42$	118.081 (22.498)	−6.7 to 5.4	0.060 (0.704)
OS $n = 46$	37.409 (8.031)	−1.0 to 2.8	0.089 (0.556)	OS $n = 42$	32.607 (7.664)	−1.3 to 3.5	0.402 (0.008)*
RPE $n = 48$	27.325 (5.091)	−0.9 to 2.9	0.210 (0.152)	RPE $n = 49$	25.753 (5.807)	−1.7 to 2.2	−0.117 (0.424)
OS and RPE $n = 48$	62.575 (13.377)	−2.5 to 3.1	0.484 (0.000)*	OS and RPE $n = 49$	53.898 (16.927)	−2.9 to 2.1	0.647 (0.000)*

The higher-quality scan was always analyzed first so that any bias due to image quality could be detected. Dashes indicate not calculated, as there were an insufficient number of control subjects in which these layers were present.

* Significant at a value $P < 0.05$.

the junction between the OS and RPE in the control group ($P = 0.029$).

We attempted to improve the reliability of measurements of these retinal layers, by performing combined measurements of the retinal layers where it was apparent that there were difficulties with delineating their borders. This affected the GCL-IPL layers, the ONL-IS layers, and the OS-RPE layers. Assessment of these combined layers was consistent on test-retest analysis with ICCs of 0.870, 0.931, and 0.933, respectively, for the nystagmus group. The ICCs were 0.931 and 0.870 for the combined ONL-IS layer and combined OS-RPE layers, respectively, in the control group. This is a strategy that potentially could be used to improve reliability when using HH-OCT to quantify normal retinal development, identify retinal pathology, and in developing objective OCT-based predictors of visual acuity.

Another factor to consider is that the subjective nature of the manual segmentation of the inner retinal layers may have contributed to the reduction in the reproducibility of the measurements of the inner retinal layers. The development of automated retinal layer segmentation and quantification software may help to further improve the reliability of the HH-OCT by removing this factor.

There was a trend toward a larger estimate of CMT measurements in the control group, OS measurement in the nystagmus group, and combined OS and RPE measurements in both the nystagmus and control groups with higher-quality images. This may be accounted for by the increased reflectance of the RPE border and IS/OS junction in the higher-quality images, which make the RPE and OS appear thicker. The trend toward a larger estimate of measurement of the INL and OPL on lesser-quality images may be explained by low reflectivity of the borders of these layers leading to an overestimation of thickness of these layers as their borders are not clearly delineated. The effects of image quality on the reliability of these measurements need to be taken into account if the HH-OCT is potentially going to be used in a clinically diagnostic and monitoring role in children with retinal conditions.

It has been previously shown that human foveal development as visualized by spectral-domain OCT correlates anatomically with histologic specimens.[21,22] Accurate assessment of foveal morphology is important, as the HH-OCT will likely play an increasingly important diagnostic and prognostic role in infants and young children with nystagmus and other eye diseases, such as ROP and glaucoma. Reliability between measurements will allow accurate monitoring of both normal and abnormal foveal development.

A limitation of this study is that our analysis was limited to the central foveal B-scan. The Bioptigen HH-OCT does not provide automatic motion stabilization to compensate for eye and head movements or movement of the probe when sampling. Consequently, the ability to successfully acquire a volumetric data sequence is much lower compared with adults. In addition, it has been shown that image inversion using spectral-domain OCT optimizes both the choroidal detail visualized and the choroidal thickness measurements obtained.[23] In the future, it would be interesting to also evaluate the test–retest reliability of this image inversion technique using the Bioptigen HH-OCT.

In this study, we have shown that the reliability of quantitative central macular thickness and photoreceptor outer segment length measurements using the HH-OCT in children are excellent and is comparable with adult OCT.[12] An OCT-based structural grading system for foveal hypoplasia has been developed previously showing that the grade of arrested foveal development is correlated with visual acuity in a range of disorders associated with foveal hypoplasia.[24] The reliability of the measurement of the length of the photoreceptor outer segment is important, as this is a strong predictor of visual acuity in albinism[11] and potentially could help predict visual acuity in various other diseases. Our results provide an important basis for future use of OCT in infants and young children for research and clinical application. In future studies, it would be important, for example, to analyze whether foveal morphology on OCT scans could be used to possibly predict visual acuity in preverbal children, especially as OS have been shown very reliable. Our results support that OCT can be used reliably clinically in young children, in diseases including foveal hypoplasia, or can be used to monitor retinal dystrophies, especially in view of imminent genetic therapy.

Acknowledgments

Supported by Medical Research Council, London, UK (MR/J004189/1); Ulverscroft Foundation, Leicester, UK; and Nystagmus Network UK.

Disclosure: **H. Lee**, None; **F. Proudlock**, None; **I. Gottlob**, None

References

1. Scott AW, Farsiu S, Enyedi LB, et al. Imaging the infant retina with a hand-held spectral-domain optical coherence tomography device. *Am J Ophthalmol*. 2009;147:364–373.e2.
2. Maldonado RS, Izatt JA, Sarin N, et al. Optimizing hand-held spectral domain optical coherence tomography imaging for neonates, infants, and children. *Invest Ophthalmol Vis Sci*. 2010;51:2678–2685.
3. Maldonado RS, O'Connell RV, Sarin N, et al. Dynamics of human foveal development after premature birth. *Ophthalmology*. 2011;118:2315–2325.
4. Maldonado RS, O'Connell R, Ascher SB, et al. Spectral-domain optical coherence tomographic assessment of severity of cystoid macular edema in retinopathy of prematurity. *Arch Ophthalmol*. 2012;130:569–578.
5. Lee AC, Maldonado RS, Sarin N, et al. Macular features from spectral-domain optical coherence tomography as an adjunct to indirect ophthalmoscopy in retinopathy of prematurity. *Retina*. 2011;31:1470–1482.
6. Vinekar A, Avadhani K, Sivakumar M, et al. Understanding clinically undetected macular changes in early retinopathy of prematurity on spectral domain optical coherence tomography. *Invest Ophthalmol Vis Sci*. 2011;52:5183–5188.
7. Chavala SH, Farsiu S, Maldonado R, et al. Insights into advanced retinopathy of prematurity using handheld spectral domain optical coherence tomography imaging. *Ophthalmology*. 2009;116:2448–2456.
8. Gerth C, Zawadzki RJ, Heon E, et al. High-resolution retinal imaging in young children using a handheld scanner and Fourier-domain optical coherence tomography. *J AAPOS*. 2009;13:72–74.
9. Lee H, Sheth V, Bibi M, et al. Potential of handheld optical coherence tomography to determine cause of infantile nystagmus in children by using foveal morphology. *Ophthalmology*. 2013;120:2714–2724.
10. Thomas MG, Kumar A, Kohl S, et al. High-resolution in vivo imaging in achromatopsia. *Ophthalmology*. 2011;118:882–887.
11. Mohammad S, Gottlob I, Kumar A, et al. The functional significance of foveal abnormalities in albinism measured using spectral-domain optical coherence tomography. *Ophthalmology*. 2011;118:1645–1652.
12. Thomas MG, Kumar A, Thompson JR, et al. Is high-resolution spectral domain optical coherence tomography reliable in nystagmus? *Br J Ophthalmol*. 2013;97:534–536.

13. Dorn EM, Hendrickson L, Hendrickson AE. The appearance of rod opsin during monkey retinal development. *Invest Ophthalmol Vis Sci*. 1995;36:2634–2651.
14. Hendrickson A, Kupfer C. The histogenesis of the fovea in the macaque monkey. *Invest Ophthalmol Vis Sci*. 1976;15:746–756.
15. Hendrickson A. A morphological comparison of foveal development in man and monkey. *Eye (Lond)*. 1992;6:136–144.
16. Hendrickson AE, Yuodelis C. The morphological development of the human fovea. *Ophthalmology*. 1984;91:603–612.
17. Yuodelis C, Hendrickson A. A qualitative and quantitative analysis of the human fovea during development. *Vision Res*. 1986;26:847–855.
18. Abramov I, Gordon J, Hendrickson A, et al. The retina of the newborn human infant. *Science*. 1982;217:265–267.
19. Dubis AM, Costakos DM, Subramaniam CD, et al. Evaluation of normal human foveal development using optical coherence tomography and histologic examination. *Arch Ophthalmol*. 2012;130:1291–1300.
20. Spaide RF, Curcio CA. Anatomical correlates to the bands seen in the outer retina by optical coherence tomography: literature review and model. *Retina*. 2011;31:1609–1619.
21. Hendrickson A, Possin D, Vajzovic L, et al. Histologic development of the human fovea from midgestation to maturity. *Am J Ophthalmol*. 2012;154:767–778.e2.
22. Vajzovic L, Hendrickson AE, O'Connell RV, et al. Maturation of the human fovea: correlation of spectral-domain optical coherence tomography findings with histology. *Am J Ophthalmol*. 2012;154:779–789.e2.
23. Lin P, Mettu PS, Pomerleau DL, et al. Image inversion spectral-domain optical coherence tomography optimizes choroidal thickness and detail through improved contrast. *Invest Ophthalmol Vis Sci*. 2012;53:1874–1882.
24. Thomas MG, Kumar A, Mohammad S, et al. Structural grading of foveal hypoplasia using spectral-domain optical coherence tomography a predictor of visual acuity? *Ophthalmology*. 2011;118:1653–1660.

Investigative Ophthalmology & Visual Science